



Transition Metal Chlorides NiCl₂, KNiCl₃, Li₆VCl₈ and Li₂MnCl₄ as Alternative Cathode Materials in Primary Li Thermal Batteries

Kyriakos Giagloglou,¹ Julia L. Payne,¹ Christina Crouch,² Richard K. B. Gover,² Paul A. Connor,¹ and John T. S. Irvine^{1,*}

¹University of St. Andrews, School of Chemistry, St Andrews Fife, KY16 9ST United Kingdom

²AWE Plc, Aldermaston, Reading RG7 4PR, United Kingdom

Transition metal chlorides KNiCl₃, Li₆VCl₈ and Li₂MnCl₄ were synthesized by solid state reaction in sealed quartz tubes and investigated as candidate cathode materials along with NiCl₂ in Li thermal batteries. The structure and morphology were studied and electrochemical properties probed at high temperatures (400°C–500°C) against Li₁₃Si₄ by galvanostatic discharge and galvanostatic intermittent titration technique (GITT). All the transition metal chlorides reduced to metal and the products of the discharge mechanism were confirmed by powder X-ray diffraction. NiCl₂ was tested at 500°C and a capacity of 360 mAhg⁻¹ was achieved. KNiCl₃ was tested at different current densities from 15 mA/cm² to 75 mA/cm² and a high voltage profile 2.30V was achieved at 425°C with a capacity of 262 mAhg⁻¹. Li₆VCl₈ was tested at 500°C and a 1.80V voltage plateau at a current density of 7.5 mA/cm² was achieved with a capacity of 145 mAhg⁻¹. Li₂MnCl₄ was tested at the same current density at 400°C and a capacity of 254 mAhg⁻¹ was achieved. These transition metal chlorides exhibit higher voltage against Li₁₃Si₄ and, hence, provide more specific power compared to the well-known metal disulfides MS₂ (M = Fe, Co, Ni) and may be promising cathode materials for Li thermal batteries.

© The Author(s) 2018. Published by ECS. This is an open access article distributed under the terms of the Creative Commons Attribution 4.0 License (CC BY, <http://creativecommons.org/licenses/by/4.0/>), which permits unrestricted reuse of the work in any medium, provided the original work is properly cited. [DOI: 10.1149/2.1231814jes]



Manuscript received August 16, 2018. Published November 14, 2018.

Thermal batteries were first designed by German scientists during World War II for V2 rockets as a military application.¹ Thermal batteries are electrochemical systems and convert directly the chemical energy into electrical energy as the anode is oxidized and the cathode is reduced utilizing a molten salt electrolyte at high temperature (>300°C). These batteries are useful due to their ability to be stored for decades before being used.² Currently, the most studied thermal batteries use a lithium alloy as an anode, a halide salt eutectic bound in an insulating porous material as an electrolyte, and a transition metal sulfide as a cathode.³ To the best of our knowledge, few transition metal chlorides have been studied as components of Li thermal batteries. Some transition metal chlorides such as NiCl₂, FeCl₂ and SbCl₃ have been studied for use as cathodes for thermal batteries in the Na/NaAlCl₄ system which used a liquid-Na anode and a NaAlCl₄ electrolyte.^{4–11} FeCl₃ was tested as cathode at temperatures where the electrolyte was solid.¹² CuCl₂, FeCl₂ and MoCl₅ were studied at 200°C as the NaAlCl₄ electrolyte melts at 152°C.¹³ Also some transition metal fluorides such as CuF₂, AgF₂, FeF₂, CrF₃ and FeF₃ were studied in the Li-alloy/LiF-KF/MF_x system or Li-alloy/LiF-NaF-KF/MF_x system.^{14,15}

This work uses the Li₁₃Si₄ alloy as an anode because it has the highest Li content and exhibits minimum oxidation under dry-room conditions.¹⁶ The discharge mechanism of Li₁₃Si₄ to Li₇Si₃ at a potential of 0.157 V against Li metal at 415°C corresponds to a capacity of 485 mA h g⁻¹.¹⁶ The LiCl-KCl eutectic (with a melting point of around 354°C) is used as the electrolyte and requires minimum 35 wt% MgO as the separator.

This work focuses on NiCl₂, KNiCl₃, Li₆VCl₈ and Li₂MnCl₄ as alternative cathode materials for use in Li thermal batteries. These materials have not been reported as cathodes in the past against Li₁₃Si₄. KNiCl₃ crystallizes in hexagonal *P6₃mc* with cell dimensions *a* = *b* = 11.795 Å and *c* = 5.926 Å as shown in Figure 1a.¹⁷ Li₂MnCl₄ adopts an inverse spinel structure (*Fd $\bar{3}$ m*, *a* = 10.502 Å) with half of the lithium ions tetrahedrally coordinated by chlorine ions and the remaining Li atoms, together with the Mn ions, are distributed statistically over the occupied octahedral sites¹⁸ as shown in Figure 1b. Li₆VCl₈ crystallizes in cubic *Fm $\bar{3}$ m* with cell parameter *a* = 10.294 Å and the structure is shown in Figure 1c.¹⁹ NiCl₂ crystallizes

in trigonal *R $\bar{3}$ m* with cell parameter *a* = *b* = 3.483 Å and *c* = 17.40 Å as shown in Figure 1d.²⁰

Experimental

Transition metal chlorides were synthesized by solid state reactions in sealed evacuated quartz tubes to ensure they were not oxidized. 0.73 g of KCl (Aldrich, 99%) and 1.27 g of NiCl₂ (Alfa Aesar, 99%) powders were used to synthesize KNiCl₃. 0.81 g of LiCl (Alfa Aesar, 99%) and 1.19 g of MnCl₂ (Strem, 97%) powders were used to synthesize Li₂MnCl₄. 1.18 g of VCl₂ (VCl₃, Aldrich, 97%) and 0.82 g of LiCl (Alfa Aesar, 99%) powders were used to synthesize Li₆VCl₈. VCl₂ was prepared through the decomposition of VCl₃ to VCl₂ under nitrogen flow at 797°C followed by a further firing of VCl₂ at 827°C for 12 hours with in a quartz tube. The powders were weighed out in the required stoichiometry for KNiCl₃, Li₆VCl₈ or Li₂MnCl₄ and mixed in a mortar and pestle in an argon filled glove box, then sealed into evacuated quartz tubes (10⁻³ mbar). The samples were heated in a tube furnace, with a heating and cooling rate of 1°C min⁻¹. KNiCl₃ was fired at 675°C, Li₂MnCl₄ was fired at 600°C and Li₆VCl₈ was fired at 800°C for 1 week. Room temperature powder X-ray diffraction data were collected using a Panalytical Empyrean diffractometer in Bragg-Brentano geometry with a Ge (220) monochromator and Cu K α radiation (λ = 1.5406 Å). Data were collected from 5° to 70° 2 θ for 1 hour with a step size of 0.017° and a time per step of 0.94 seconds. WinXPOW software was used for indexing and refining the unit cell parameters. Scanning electron microscopy was carried out using a Jeol JSM-5600 model microscope. Composite cathode pellets for high temperature electrochemical investigations were made by mixing 75 wt% NiCl₂, KNiCl₃, Li₆VCl₈ or Li₂MnCl₄ (0.15 g) with 25 wt% Super P Carbon (0.05 g) and pressing in a 13 mm diameter die. The anode pellet was made by mixing 75 wt% Li₁₃Si₄ (Lithium Rockwood) (0.15 g) and 25 wt% LiCl-KCl (0.05 g) electrolyte. The amount of anode (0.15 g) is in excess to keep the discharge on the first anode plateau for the amount of cathode used. Thermal batteries were assembled in an argon-filled glove box by stacking a separator pellet containing 45 wt% MgO and 55 wt% LiCl-KCl eutectic (Sigma Aldrich 99.99%) electrolyte (0.2 g) onto an anode pellet and then placing the cathode pellet on the top. To prevent movement all three pellets were contained in a ceramic cup. Graphite foil was used as the top and bottom current collectors. The resulting cell was placed into a Swagelok sample holder, allowing the measurements to be carried out sealed under argon. The resulting assembly (comprising of

*Electrochemical Society Member.

^zE-mail: jtsi@st-andrews.ac.uk

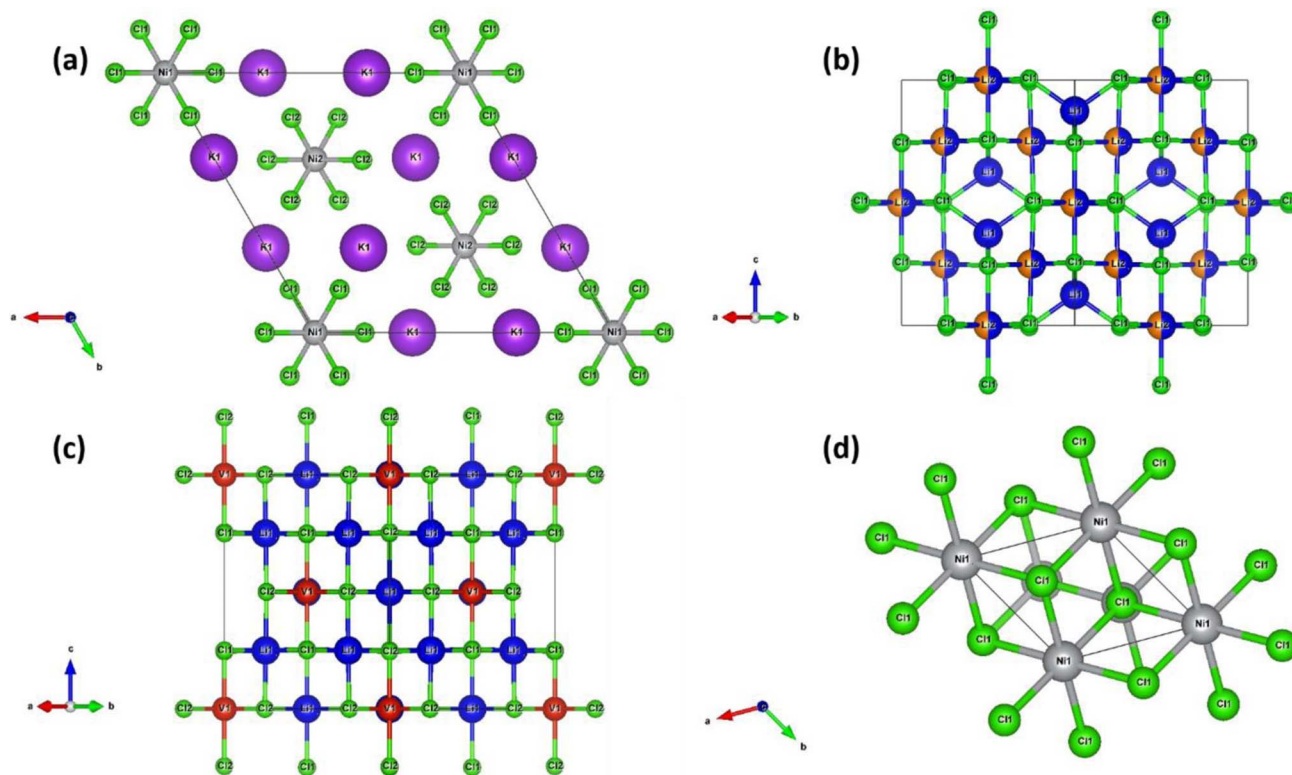


Figure 1. Crystal structure of (a) KNiCl_3 , (b) Li_2MnCl_4 , (c) Li_6VCl_8 and (d) NiCl_2 . Purple atoms are potassium, green atoms are chlorine, gray atoms are nickel, blue atoms are lithium, orange atoms are manganese and red atoms are vanadium.

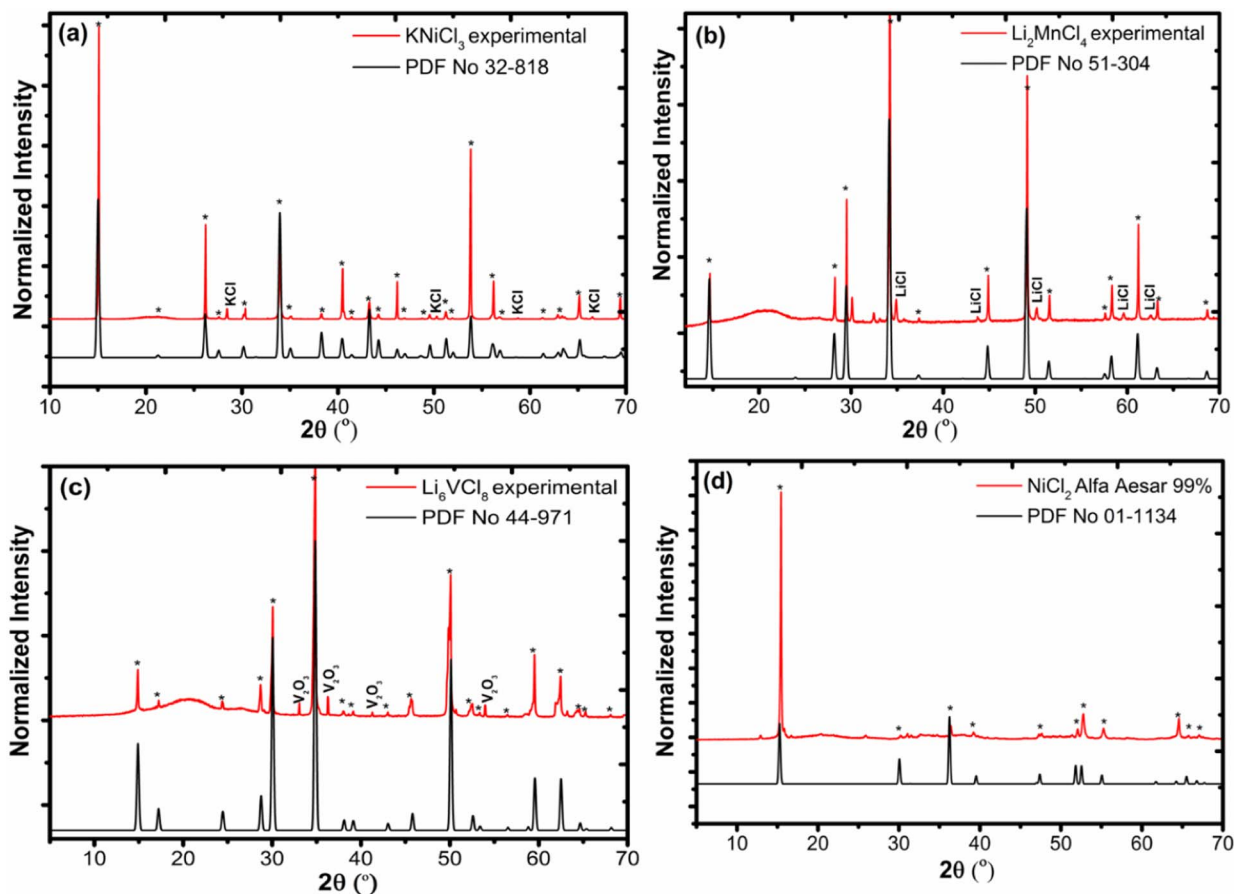


Figure 2. PXRD data of (a) KNiCl_3 , (b) Li_2MnCl_4 , (c) Li_6VCl_8 and (d) NiCl_2 . Experimental patterns are shown by the red line and the simulated diffraction patterns using published crystallographic models are shown by the black line.

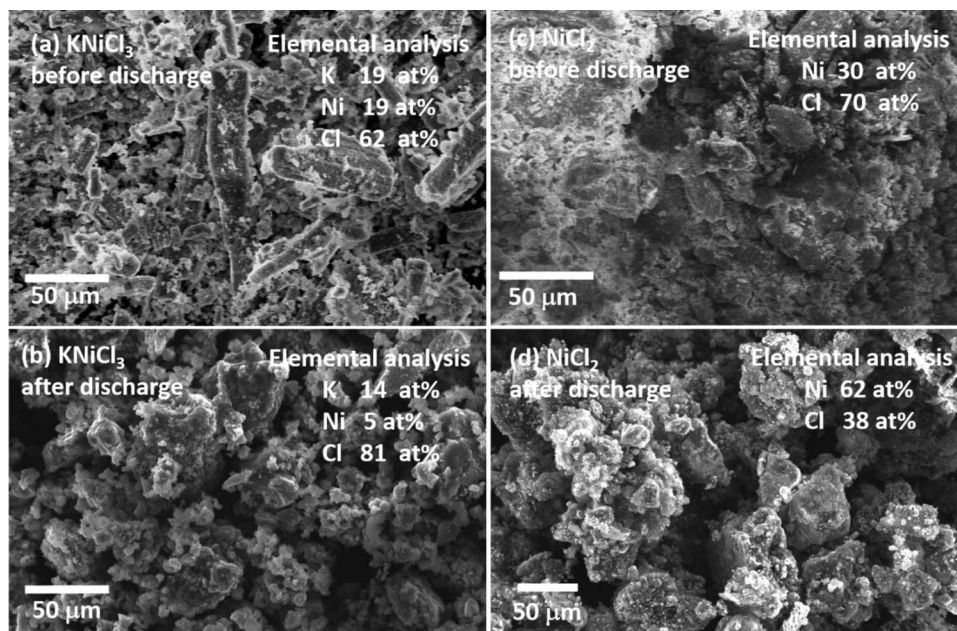


Figure 3. SEM images of KNiCl_3 and NiCl_2 before and after discharge.

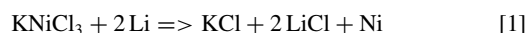
the cell within the Swagelok sample holder) was heated, and during this procedure the electrolyte melts and the voltage starts to rise. The thermal batteries were tested at high temperatures (NiCl_2 and Li_6VCl_8 at 500°C , KNiCl_3 at 425°C and LiMnCl_4 at 400°C) using a Maccor battery tester (model 5300) by galvanostatic discharge and galvanostatic intermittent titration technique (GITT). In the GITT method, galvanostatic discharge pulses, each 10 minutes long, followed by 5 minutes of relaxation time, with no current passing through the cell show the potential which drops between the pulses and the relaxation until a potential of 0.5 V is reached. The experimental capacity was calculated using the Maccor software and then this was converted to x , the moles of lithium ions per moles of formula unit.

Results and Discussion

Cathode materials characterization.— NiCl_2 , KNiCl_3 , Li_6VCl_8 and Li_2MnCl_4 were analyzed by powder X-ray diffraction and the resulting diffraction patterns are shown in Figure 2. In the synthesis of Li_6VCl_8 the main phase corresponded to Li_6VCl_8 but there is also a V_2O_3 impurity ($a = 4.948(7) \text{ \AA}$, $c = 13.989(20) \text{ \AA}$). As the synthesis of Li_6VCl_8 was in a sealed quartz tube we suggest that the V_2O_3 arises as an impurity in the synthesis of the VCl_2 reagent during the decomposition VCl_3 to VCl_2 . KNiCl_3 was identified as the main phase but there is also a KCl impurity ($a = 6.280(25) \text{ \AA}$). Li_2MnCl_4 was identified as the main phase but there is a LiCl impurity ($a = 5.140(10) \text{ \AA}$). NiCl_2 (Alfa Aesar, 99%) was identified as the main phase. The unit cell parameters of NiCl_2 , KNiCl_3 , Li_2MnCl_4 and Li_6VCl_8 are given in Table I. All the materials were studied electrochemically with the impurities (LiCl and KCl) as the electrolyte LiCl-KCl eutectic which is used, consists of KCl and LiCl . The morphology and the elemental composition of the materials was investigated by SEM and EDX before and after discharge and results are shown in Figures 3 and 4. The SEM images show that the morphology has been changed after the discharge and the size of the crystallites differs for each material. EDX confirms K 19 at%, Ni 19 at% and Cl 62 at% as expected for KNiCl_3 and Ni 30 at%, Cl 70 at% as expected for NiCl_2 before testing. The elemental analysis of both KNiCl_3 and NiCl_2 cathodes after testing (K 14 at%, Ni 5 at%, Cl 81 at% and Ni 62 at%, Cl 38 at%, respectively) means different products of the electrochemical mechanism as Ni metal, KCl and LiCl .

Electrochemical investigation of transition metal chlorides at high temperature.—Galvanostatic discharge curves for measure-

ments carried out at 425°C and a galvanostatic intermittent titration technique curve for a measurement at 425°C for KNiCl_3 are presented in Figure 5. Galvanostatic discharge was performed at different current densities from 15 mA/cm^2 to 75 mA/cm^2 . At current densities of 15, 30 and 60 mA/cm^2 there is a high cell voltage (over than 2.0 V) but a flat voltage plateau could not be obtained as we are getting an insertion reaction rather than a conversion reaction. A voltage plateau is preferred as this gives a better voltage control during the discharge reaction. A capacity of 262 mA h g^{-1} was measured for KNiCl_3 and this corresponds to a value of $x = 2$ for the number of lithium atoms transferred during the discharge process. At current densities of 68 and 75 mA/cm^2 the cell voltage is lower which is probably due to a higher cell resistance. The electrochemical mechanism corresponds to



This electrochemical Reaction 1 is expected as it is analogous to the system $\text{Na/NaAlCl}_4/\text{NiCl}_2$.⁶ The galvanostatic intermittent titration technique measurements (GITT) show the IR drop is 125 mV at the beginning of discharge and 375 mV at the end of the measurement, which indicates that the cell resistance is increasing during the reduction of the cathode, from a resistance of 16Ω at the beginning of the measurement to 50Ω after the cell discharge, which suggests that it is more difficult for the lithium ions to transfer from the anode to the cathode electrode.

Galvanostatic discharge curves for measurements carried out at 400°C and the galvanostatic intermittent titration technique curve for measurements carried out at 400°C for Li_2MnCl_4 are presented in Figure 6. Galvanostatic discharge was performed at different current densities from 15 mA/cm^2 to 75 mA/cm^2 . At a current density of 15 mA/cm^2 there is a high cell voltage (2.50 V) similar to KNiCl_3 but again a flat voltage plateau could not be obtained. Li_2MnCl_4 exhibits a

Table I. Refined unit cell parameters of transition metal chlorides.

Unit cell [\AA]	Experimental	Published
a and c KNiCl_3	11.800(11) and 5.926(4)	11.795 and 5.926 ¹⁷
a Li_2MnCl_4	10.495(7)	10.502 ¹⁸
a Li_6VCl_8	10.294(5)	10.294 ¹⁹
a and c NiCl_2	3.468(21) and 17.30(7)	3.483 and 17.40 ²⁰

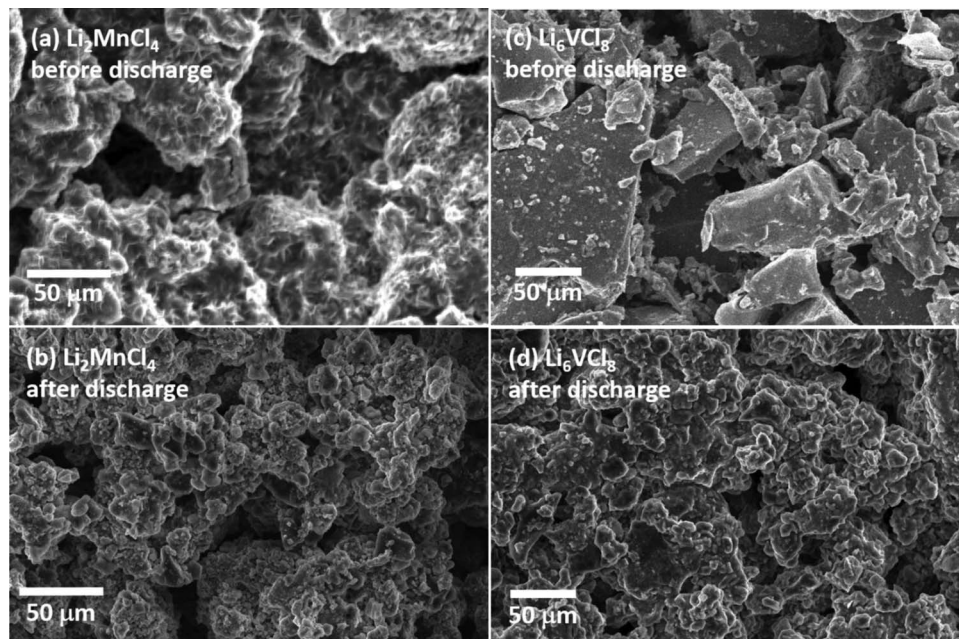


Figure 4. SEM images of Li_2MnCl_4 and Li_6VCl_8 before and after discharge.

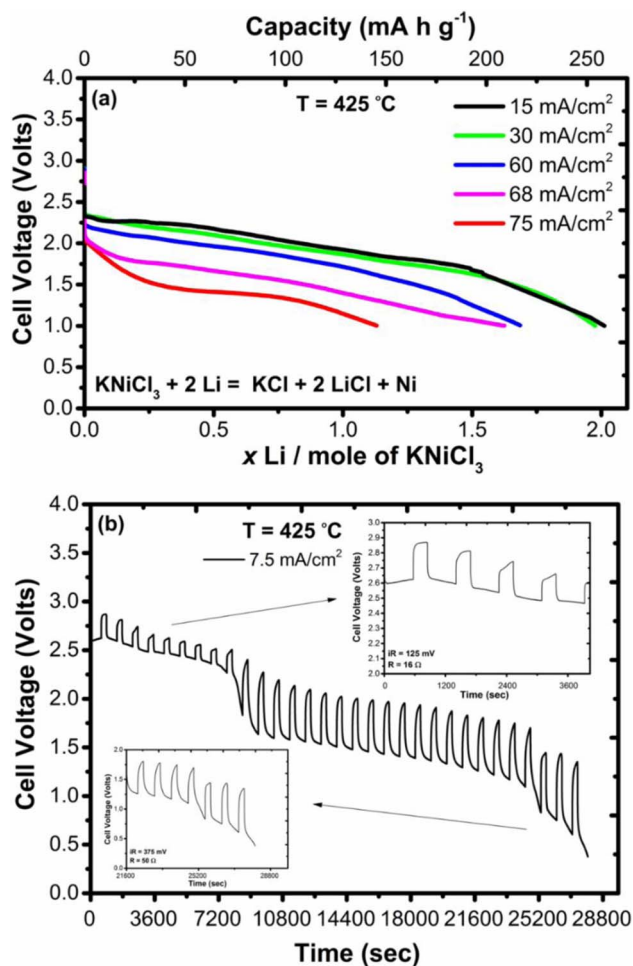


Figure 5. (a) Galvanostatic discharge of KNiCl_3 at current densities of 15, 30, 60, 68 and 75 mA/cm^2 at 425 °C and (b) galvanostatic intermittent titration technique of KNiCl_3 at current density of 7.5 mA/cm^2 at 425 °C.

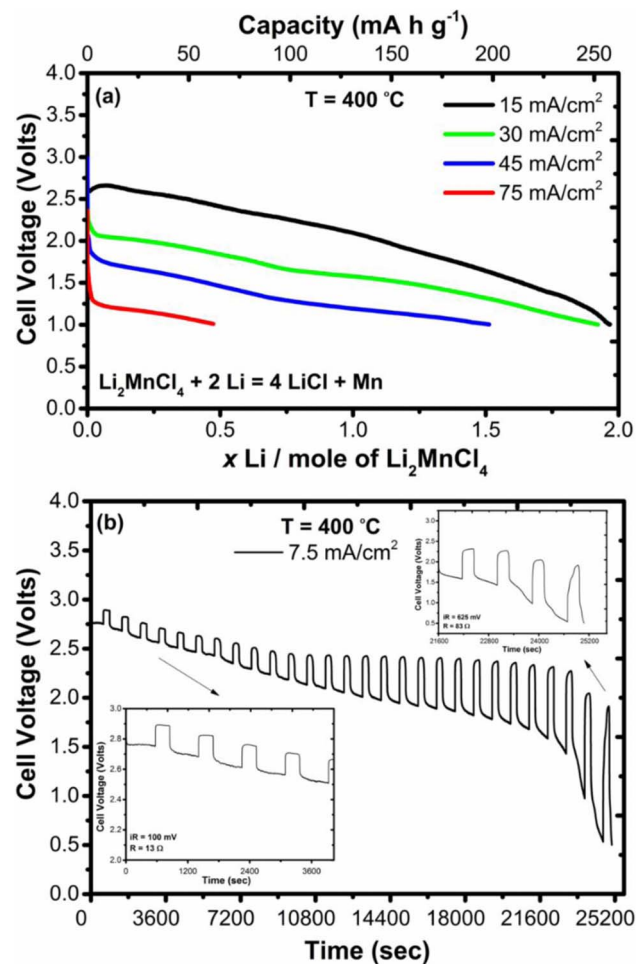


Figure 6. (a) Galvanostatic discharge of Li_2MnCl_4 at current densities of 15, 30, 45 and 75 mA/cm^2 at 400 °C and (b) galvanostatic intermittent titration technique of Li_2MnCl_4 at current density of 7.5 mA/cm^2 at 400 °C.

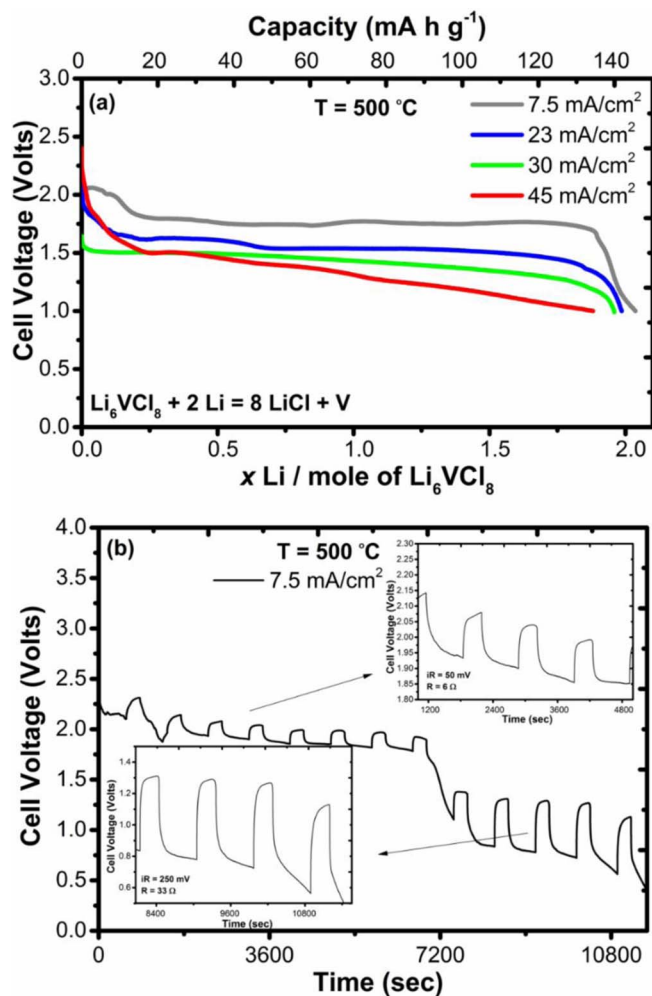


Figure 7. (a) Galvanostatic discharge of Li_6VCl_8 at current densities of 7.5, 23, 30 and 45 mA/cm^2 at 500°C and (b) galvanostatic intermittent titration technique of Li_6VCl_8 at current density of 7.5 mA/cm^2 at 500°C .

maximum capacity of 254 mA h g^{-1} . The electrochemical mechanism corresponds to



The IR drop is 100 mV at the beginning of discharge and 625 mV at the end of the measurement, which indicates that the cell resistance is increasing from a resistance of 13 Ω at the beginning of the measurement to 83 Ω after the cell discharge.

Galvanostatic discharge curves for measurements were carried out at 500°C and the galvanostatic intermittent titration technique curve for a measurement carried out at 500°C for Li_6VCl_8 is presented in Figure 7. Galvanostatic discharge was performed at different current densities from 7.5 mA/cm^2 to 45 mA/cm^2 . At a current density of 7.5 mA/cm^2 there is a flat voltage profile at 1.80 V and a capacity of 145 mA h g^{-1} was achieved. At current densities of 23 and 30 mA/cm^2 , Li_6VCl_8 shows a lower but again flat voltage plateau at 1.50 V. However at a current density of 45 mA/cm^2 a flat voltage plateau could not be obtained. Therefore, at low current densities, the behavior of Li_6VCl_8 is different to that of Li_2MnCl_4 and KNiCl_3 as Li_6VCl_8 is the only material which exhibits a flat voltage plateau in the discharge profile. The electrochemical mechanism corresponds to



The cell resistance increases during the reduction of the cathode from 6 Ω at the beginning to 33 Ω at the end of discharge.

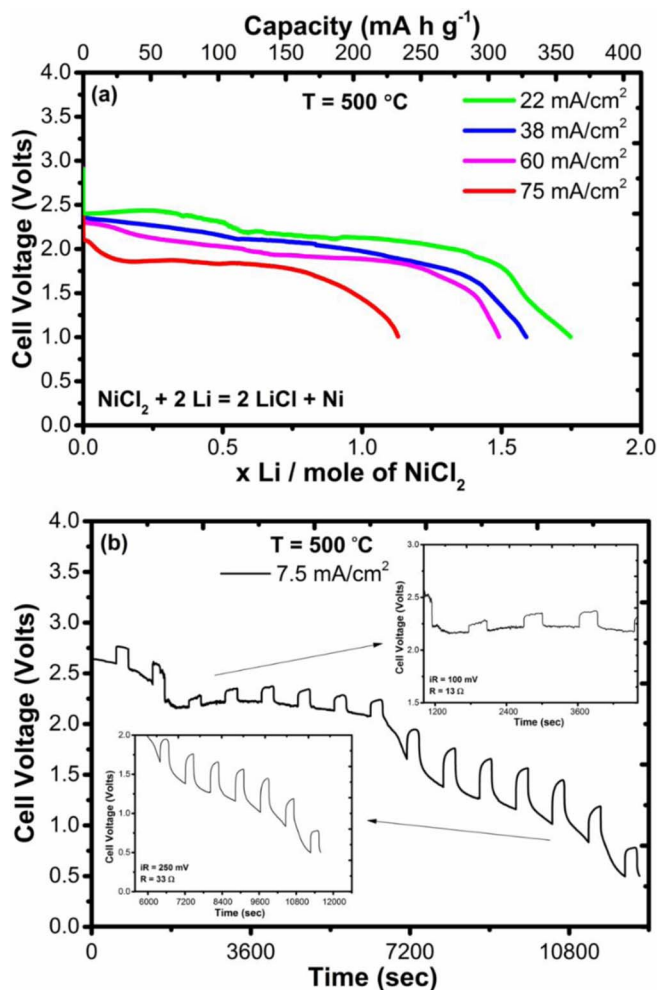
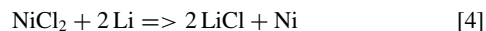


Figure 8. (a) Galvanostatic discharge of NiCl_2 at current densities of 22, 38, 60 and 75 mA/cm^2 at 500°C and (b) galvanostatic intermittent titration technique of NiCl_2 at current density of 7.5 mA/cm^2 at 500°C .

Galvanostatic discharge curves for measurements carried out at 500°C and the galvanostatic intermittent titration technique curve for a measurement carried out at 500°C for NiCl_2 are presented in Figure 8. Galvanostatic discharge was performed at different current densities from 22 mA/cm^2 to 75 mA/cm^2 . At a current density of 22 mA/cm^2 there is a high voltage profile at 2.25 V and a capacity of 360 mA h g^{-1} was achieved. At current densities of 60 and 75 mA/cm^2 , NiCl_2 shows a lower voltage profile but still at around 2.0 V. The electrochemical mechanism corresponds to



The cell resistance increases during the reduction of the cathode from 13 Ω at the beginning to 33 Ω at the end of discharge.

The advantage of transition metal chlorides is that they provide more specific power and exhibit higher voltage against $\text{Li}_{13}\text{Si}_4$ at high temperatures compared to that of the well-known metal disulfides FeS_2 , CoS_2 and NiS_2 as shown in Table II. The thermal stability and the overall capacity of transition metal chlorides in the voltage range from OCV 3.0 V to 1.50 V are also comparable to that of the most commonly used disulfides.

PXRD data were collected after discharge for all of the cathodes as shown in Figure 9. The product of the electrochemical reaction of KNiCl_3 is KCl ($a = 6.292(3) \text{ \AA}$), Ni metal ($a = 3.524(7) \text{ \AA}$) and LiCl as shown in Figure 9a. There are some peaks of the starting material KNiCl_3 ($a = 11.805(4) \text{ \AA}$ and $c = 5.935(12) \text{ \AA}$) and some peaks of NiO ($a = 4.177(4) \text{ \AA}$).

Table II. Overall capacity, thermal stability, voltages vs Li_3Si_4 , and specific power of transition metal chlorides compared to transition metal disulfides FeS_2 , CoS_2 and NiS_2 .

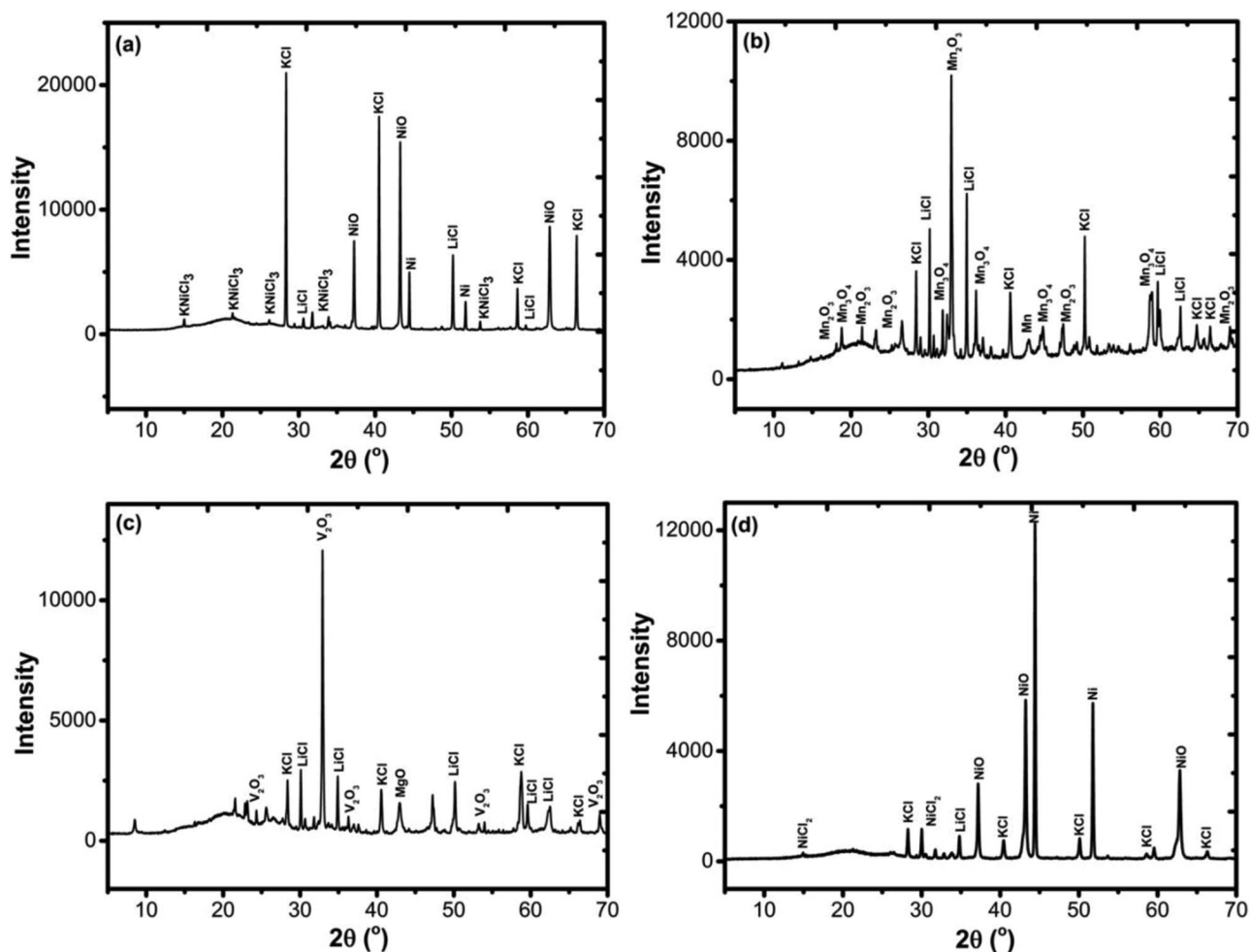
Sulfides	Overall Capacity (mA h g^{-1})	Thermal Stability $^{\circ}\text{C}$	Voltages vs Li_3Si_4	Capacity (mA h g^{-1}) in the voltage range (OCV – 1.5 V)	Specific power (W h g^{-1})
				Voltage window ~ 0.5 V	
FeS_2	558 ³	580 ^{24,25}	1.77 V, 1.64 V, 1.13 V ²¹	357	0.14 ²⁶
CoS_2	598 ³	650 ²²	1.75 V, 1.40 V, 1.25 V ²¹	348	0.11 ²⁷
NiS_2	545 ³	600 ²³	1.76 V, 1.60 V, 1.40 V, 1.25 V ²¹	349	≥ 0.11 ²⁸
Chlorides				Voltage window ~ 1.5 V	
NiCl_2	360	500	2.25 V	326	0.80
KNiCl_3	262	675	2.25 V	215	0.51
Li_6VCl_8	145	800	1.80 V	136	0.26
Li_2MnCl_4	254	600	2.50 V	214	0.54

The product of the electrochemical reaction of Li_2MnCl_4 is LiCl ($a = 5.142(17)$ Å) and Mn metal ($a = 8.948(2)$ Å) as shown in Figure 9b. There are some peaks of the electrolyte KCl and peaks of Mn_2O_3 ($a = 9.44(5)$ Å, $b = 9.55(4)$ Å and $c = 9.28(3)$ Å) and Mn_3O_4 ($a = 5.747(3)$ Å and $c = 9.444(6)$ Å).

The product of the electrochemical reaction of Li_6VCl_8 is LiCl ($a = 5.139(12)$ Å) with some residual V_2O_3 ($a = 4.944(15)$ and $c = 14.020(4)$ Å) as shown in Figure 9c. There are also peaks of

KCl ($a = 6.289(3)$ Å) and MgO ($a = 4.209(12)$ Å) and some other peaks that were difficult to identified and indexed to the known PDF database.

The product of the electrochemical reaction of NiCl_2 is LiCl ($a = 5.129(5)$ Å) and Ni metal ($a = 3.524(7)$ Å) as shown in Figure 9d. There are some peaks of the starting material NiCl_2 ($a = 3.468(21)$ Å and $c = 17.302(7)$ Å), some peaks of NiO ($a = 4.180(12)$ Å) and some peaks of KCl ($a = 6.299(18)$ Å).

**Figure 9.** PXRD data of the cathode after galvanostatic discharge of (a) KNiCl_3 , (b) Li_2MnCl_4 , (c) Li_6VCl_8 and (d) NiCl_2 .

We attribute the small amount of oxide impurity in each of the diffraction patterns after discharge to a small amount of oxidation of the sample prior to and during the collection of PXRD data.

Conclusions

The high temperature discharge behavior of transition metal chlorides NiCl_2 , KNiCl_3 , Li_2MnCl_4 and Li_6VCl_8 synthesized by solid state reaction (except NiCl_2) is presented in this work. At temperatures of 400°C – 500°C the value of the working voltage profile was recorded at different current densities. KNiCl_3 exhibits a high cell voltage at 425°C vs $\text{Li}_{13}\text{Si}_4$ but not a flat voltage profile and a capacity of 262 mA h g^{-1} was achieved. Li_2MnCl_4 was tested at 400°C and a capacity of 254 mA h g^{-1} was achieved. Li_6VCl_8 exhibits a flat voltage plateau of 1.80 V at a current density of 7.5 mA/cm^2 with capacity of 145 mA h g^{-1} . NiCl_2 exhibits a high voltage profile of 2.25 V at a current density of 22 mA/cm^2 with capacity of 360 mA h g^{-1} . These transition metal chlorides provide more specific power and exhibit higher voltage against $\text{Li}_{13}\text{Si}_4$ compared to that of the well-known metal disulfides so we suggest transition metal chlorides as alternative promising candidate materials for Li thermal battery applications.

Acknowledgments

Special thanks to AWE Plc for their support and funding for this work. The authors would also like to acknowledge the EPSRC Platform grant EP/K015540/1 and the Royal Society Wolfson Merit Award WRMA 2012/R2.

ORCID

John T. S. Irvine  <https://orcid.org/0000-0002-8394-3359>

References

- W. E. Kuper, *Proceedings of 36th Power Sources Conference* 300 (1994).
- R. A. Guidotti and P. Masset, *J. Power Sources*, **161**, 1443 (2006).
- S. K. Preto, Z. Tomczuk, S. von Winbush, and M. F. Roche, *J. Electrochem. Soc.*, **130**, 264 (1983).
- J. Prakash, L. Redey, D. R. Vissers, and J. De Gruson, *J. Appl. Electrochem.*, **30**(11), 1229 (2000).
- J. Prakash, L. Redey, and D. R. Vissers, *J. Electrochem. Soc.*, **147**(2), 502 (2000).
- R. C. Galloway, *J. Electrochem. Soc.*, **134**(1), 256 (1987).
- C.-L. Yu, J. Winnick, and P. A. Kohl, *J. Electrochem. Soc.*, **138**(1), 339 (1991).
- J. Coetzer, *J. Power Sources*, **18**, 377 (1986).
- R. J. Bones, D. A. Teagle, S. D. Brooker, F. L. Cullen, and J. Lumsdon, *Proceedings of the Extended Abstracts of the Spring Meeting of The Electrochemical Society*, **87**(1), 786 (1987).
- K. T. Adendorff and M. M. Thackeray, *J. Electrochem. Soc.*, **135**(9), 2121 (1988).
- J. L. Sudworth, in: M. Barak, (Ed.), "High temperature batteries", in *Electrochemical Power Sources, Primary and Secondary Batteries*, Peter Peregrinus, Ltd., NY, IEE Energy Series 1, 403 (1980).
- R. J. Vaughn, R. A. Carpio, and L. A. King, US Pat. 4,764,438, August 16, (1988).
- D. M. Ryan, R. A. Marsh, and R. K. Bunting, *Proceedings of the 28th Power Sources Symposium*, 90 (1978).
- J. D. Briscoe, *Proceedings of the 33rd Intersociety Engineering Conference on Energy Conversion*, Colorado Springs, CO, August 2–6, (1998).
- D. D. Briscoe and G. L. Castro, SAE Technical Paper 1999-01-1401, (1999).
- C. J. Wen and R. A. Huggins, *J. Solid State Chem.*, **37**, 271 (1981).
- D. Visser, G. C. Verschoor, and D. J. W. Ijdo, *Acta Cryst.*, **B36**, 28 (1980).
- C. J. J. Van Loon and J. De Jong, *Acta Cryst.*, **B31**, 2549 (1975).
- L. Hanebali, T. Machej, C. Cros, and P. Hagenmuller, *Materials Research Bulletin*, **16**, 887 (1981).
- A. Ferrari, A. Braibanti, and G. Bigliardi, *Acta Cryst.*, **16**, 846 (1963).
- P. J. Masset and R. A. Guidotti, *Journal of Power Sources*, **178**, 456, (2008).
- H. Rau, *J. Phys. Chem. Solids*, **37**, 931, (1976).
- R. A. Guidotti, P. J. Nigrey, F. W. Reinhardt, and J. G. Odinek, *Proceedings of the 40th Power Sources Conference*, **250**, (2002).
- M. C. Hash, J. A. Smaga, R. A. Guidotti, and F. W. Reinhardt, *Proceedings of the 8th International Symposium on Molten Salts*, **228**, (1992).
- I. C. Hoare, H. J. Hurst, W. I. Stuart, and T. J. White, *J. Chem. Soc. Faraday Trans.*, **184**(9), 3071 (1988).
- Hiroshi Shimotake and William J. Walsh, *Development of a compact, high capacity FeS₂ electrode*, Argonne National Laboratory 9700 South Cass Avenue Argonne, Illinois 60439.
- S. J. Specht and N. Schuster, *High power/high temperature battery development*, US Army Laboratory Command (LABCOM), Electronics Technology and Devices Laboratory. ATTN: SLCET-PR, Fort Monmouth, NJ 07703-5601, September (1992).
- K. M. Abraham and J. E. Elliot, *J. Electrochem. Soc.*, **131**(10), 2211, (1984).